

Ferromagnetic coupling in $\text{Nd}_x\text{Ca}_{2-x}\text{FeMoO}_6$ double perovskites: Dominant band-filling effects

D. Rubi, C. Frontera, and J. Fontcuberta

Institut de Ciència de Materials de Barcelona, CSIC, Campus Universitat Autònoma de Barcelona, E-08193 Bellaterra, Spain

M. Wojcik and E. Jedryka

Institute of Physics, Polish Academy of Sciences, Al. Lotników 32/46, 02 668 Warszawa, Poland

C. Ritter

Institute Laue Langevin, 6, Rue Jules Horowitz, F-38042 Cedex 9, Grenoble, France

(Received 22 March 2004; published 8 September 2004)

As trivalent Nd^{3+} and divalent Ca^{2+} ions have virtually the same ionic size, $\text{Nd}_x\text{Ca}_{2-x}\text{FeMoO}_6$ is a *quasi-ideal* material to explore electron-doping effects in double perovskites. We report here a study of its structural, magnetic, and transport properties. We show that although steric effects are absent and the symmetry of the structure is preserved upon Nd doping, the Curie temperature of these oxides rises at a rate of 1.8(3)K/%Nd. We argue that this is a genuine band-filling effect that takes place in a rigid electronic-band system. On the basis of these observations we critically revise some assumptions in currently available models of ferromagnetic coupling in double perovskites.

DOI: 10.1103/PhysRevB.70.094405

PACS number(s): 75.47.Gk, 75.30.-m, 76.60.Lz

I. INTRODUCTION

The double perovskites (DP) $\text{A}_2\text{BB}'\text{O}_6$ are being intensively investigated nowadays due to the finding of ferromagnetic and metallic behavior in $\text{Sr}_2\text{FeMoO}_6$ (SFMO).¹ Indeed SFMO has a Curie temperature of above 400 K and it has been predicted to be a half-metallic ferromagnet;¹ thus it is an almost ideal candidate to be used in magnetoelectronics as it overcomes the severe temperature limitations of the manganese perovskites. In the ideal $\text{Sr}_2\text{FeMoO}_6$ structure, the $\text{SrFe}(\text{Mo})\text{O}_3$ perovskite building-blocks form a NaCl-superlattice in such a way that the Fe-Fe(Mo-Mo) distance is doubled with respect to elementary perovskite unit cell. The magnetic structure of this oxide was originally¹ described as resulting from an antiferromagnetic coupling between Fe- d^5 ions (Fe^{3+}) electrons and Mo- $4d^1$ electrons, in a ferrimagnetic-like structure. However, recent reports indicating that the dominant magnetic interaction in the system is ferromagnetic^{2,3} and that magnetic moment at Mo ions is small^{4,5} have forced to review the picture. In fact, the observation of a substantial low-field magnetoresistance¹ and that electrical resistivity appears to be correlated with the Curie temperature⁶ suggested that charge carriers have a dominant role in the magnetic coupling. Therefore, it was assumed that the localized *spin-up* electrons of the $3d^5(\text{Fe}^{3+})$ configuration are antiferromagnetically coupled via intra-atomic Hund coupling to an itinerant *spin-down* electron shared by hybridized $3d(\text{Fe})$ - $4d(\text{Mo})$ orbitals. It follows that this picture bears some resemblance to the double-exchange model used to describe the ferromagnetic coupling in manganites. However, we note that the Mo ions, having an electronic configuration $4d^{(1-\delta)}$, are very weakly magnetic and the distance between the magnetic ions (Fe) is of about 0.7 nm. We recall that in the ferromagnetic manganites the Mn-Mn distance is ~ 0.35 nm, that is about a half of the Fe-Fe distance in DP's. In spite of this, the Curie temperature

in DP's is higher than in manganites. This simple observation indicates that the nature of the ferromagnetic coupling in DP shall differ in some essential aspects from that of manganites.

Tovar *et al.*³ proposed that the ferromagnetic coupling is mediated by the itinerant carriers (electrons) at the Fermi level much as in the conventional Ruderman-Kittel-Kasuya-Yosida (RKKY) itinerant ferromagnets or in the diluted magnetic semiconductors.⁷ From that picture, a natural suggestion to increase the Curie temperature emerged and it was proposed that increasing the carrier density may lead to a change of the density of states at the Fermi level, and a concomitant change of the Curie temperature.³ Electron doping has been achieved by substituting trivalent ions (La^{3+} or Nd^{3+}) for divalent Sr^{2+} or Ba^{2+} ions in $\text{Sr}_{2-x}(\text{La}, \text{Nd})_x\text{FeMoO}_6$ (Refs. 8–13) or $\text{Ba}_{2-x}\text{La}_x\text{FeMoO}_6$.¹⁴ Using a variety of techniques, including low-field magnetic susceptibility,^{8,14} Arrot plots¹⁵ and neutron powder diffraction,^{9,12,13} it has been shown that the Curie temperature of SFMO is increased when the carrier density increases. Moreover, photoemission experiments on $\text{Sr}_{2-x}\text{La}_x\text{FeMoO}_6$ have provided evidence of the enhancement of the density of states at the Fermi level upon La substitution.¹⁶ Nuclear magnetic resonance¹⁷ or Mössbauer spectroscopy¹⁰ have been used to show that La or Nd substitution indeed produces a carrier injection mainly at the $4d(\text{Mo})$ states. It may be useful to recall that electron doping has also been attempted in other DP's having a metallic sublattice not formed by (Fe, Mo), such as Sr_2CrWO_6 .¹⁸ The results reported so far are disappointing, in the sense that the Curie temperature of $\text{Sr}_{2-x}\text{La}_x\text{CrWO}_6$ does not increase upon La doping.¹⁸

Starting from a double-exchange-like model, Millis *et al.*¹⁹ have used the dynamical mean field method to estimate the Curie temperatures of several DP's such as $\text{Sr}_2\text{FeMoO}_6$ and $\text{Ca}_2\text{FeReO}_6$. However the approximations/assumptions of the model appear to be not appropriate as $\text{Sr}_2\text{FeMoO}_6$ is

predicted to be nonferromagnetic and the Curie temperature of the Re-oxide is found to be of only 1/5 of the experimental value. More successful have been the approaches of Alonso²⁰ and Sarma²¹ as a ferromagnetic ground state is found for SFMO. The effect of electron doping has also been addressed theoretically. However, again the predictions sharply disagree with the experiments described above. Indeed, Millis¹⁹ and Alonso²⁰ have argued that in a double-exchange scenario and in absence of antisites [misplaced Fe(Mo) ions at Mo(Fe) sites], the Curie temperature should decrease if the carrier concentration is increased.

These theoretical models assume that doping occurs in a rigid-band system; that is the inter-site Fe-O-Mo hopping integrals are not modified by the doping process. However, it is clear that this assumption is quite unrealistic in the experiments reported so far. Indeed, in $A_{2-x}L_x\text{FeMoO}_6$ ($A=\text{Sr}$ or Ba ; $L=\text{La}$ or Nd) the ionic sizes of Sr^{2+} or Ba^{2+} ions (1.26 and 1.42 Å, respectively) substantially differ from the substituting ions (La^{3+} and Nd^{3+} , with 1.16 and 1.109 Å, respectively) and consequently the atomic substitution shall trigger a rotation of $(\text{Fe},\text{Mo})\text{O}_6$ octahedra. This rotation bends the mean Fe-O-Mo bond angle, and even lowers the crystal symmetry,^{8,11-13} modifying the hopping-integrals and consequently the bandwidth. To what extent this is the ultimate reason for the disagreement between experiments and theoretical predictions remains to be elucidated and this is the purpose of the present manuscript. To avoid steric modifications of the Fe-O-Mo bond topology upon lanthanide substitution we have synthesized $\text{Ca}_{2-x}\text{Nd}_x\text{FeMoO}_6$: as the ionic radius of Nd^{3+} (1.109 Å) is almost coincident with that of Ca^{2+} (1.12 Å) we do not expect substantial bond modifications upon Nd substitution. Indeed, we will show that, in contrast to previously reported substitution schemes,^{8,11-13} the symmetry of the crystal lattice is kept constant upon Nd doping. It follows that $\text{Ca}_{2-x}\text{Nd}_x\text{FeMoO}_6$ is a *quasi-ideal* material to compare doping effects with theoretical predictions.

We will report here a detailed characterization of these oxides with a special emphasis and cautions on the determination of the Curie temperature as a function of the Nd-doping. Moreover, due to the similar sizes of Nd^{3+} and Ca^{2+} ions, the structural disorder created by the substitution is expected to be very much reduced and indeed, the magnetic transition -either in magnetization or neutron powder diffraction experiments- are sharper than in previous (LaSr) or (LaNd) studies. We will show, for the first time, that electron doping in Ca-based double perovskites promotes a substantial increase of the Curie temperature (T_C). Moreover, we will show from^{95,97}Mo nuclear magnetic resonance (NMR) that e-doping strongly enhances Mo magnetic moment allowing one to conclude that doped electrons are accommodated in the spin polarized $4d$ -Mo orbitals. These findings definitely settle that carrier doping in $\text{Sr}_2\text{FeMoO}_6$ raises T_C and that discrepancies with theoretical modes probably go deeper than the rigid-band approximation. As discussed in the last part of this paper, these observations provide serious constraints to microscopic models.

II. EXPERIMENTAL

Ceramic samples of $\text{Nd}_x\text{Ca}_{2-x}\text{FeMoO}_6$, with $x=0, 0.2, 0.4, 0.6, \text{ and } 0.8$, were synthesized by standard solid-state reac-

tions. CaCO_3 , Nd_2O_3 , Fe_2O_3 , and MoO_3 were mixed in appropriate ratios and fired twice in air at 900°C . After that, the obtained powders were pressed into small pellets and a final treatment was done at 1250°C in reducing Ar-H_2 atmosphere. Finally, samples were slowly cooled down to room temperature. All samples resulted single phase, with only small traces ($<1\%$) of CaMoO_4 for $x=0.4$ and 0.8 . The structural characterization was done by means of x-ray powder diffraction (XRPD, Siemens D-5000 diffractometer, $\text{Cu } k_{\alpha 1, \alpha 2}$ radiation). Additionally, neutron powder diffraction (NPD) studies were performed at the Institute Laue-Langevin (ILL, Grenoble) at the D1B ($\lambda=2.52$ Å) diffractometer from room temperature (RT) to well above T_C . Rietveld refinements of diffraction data were done using FULLPROF software.²² XRPD and NPD data collected at RT have been jointly refined in order to determine the changes of the structural parameters upon doping.

Magnetic characterization was performed by using a Quantum-Design SQUID magnetometer (2–300 K, up to 5.5 T). Magnetic measurements above room temperature were made by using a vibrating sample magnetometer (VSM). The magnetotransport properties have been measured in a PPMS system from Quantum Design.

Microscopic characterization of charge and spin distribution around Mo has been carried out using NMR technique.^{95,97}Mo NMR experiments have been performed at 4.2 K in zero magnetic field using a coherent, phase sensitive spin echo spectrometer. The NMR spectra have been recorded every 1 MHz in the frequency range 20–140 MHz and corrected for the intrinsic enhancement factor which was experimentally determined at each frequency point from the power dependence of signal intensity.

III. RESULTS AND DISCUSSION

A. XRPD and NPD results

The diffraction patterns corresponding to $\text{Nd}_x\text{Ca}_{2-x}\text{FeMoO}_6$ (NCFMO) samples were successfully refined on the monoclinic $P2_{1/m}$ space group (SG) as was previously reported for $\text{Ca}_2\text{FeMoO}_6$ samples.²³ It is well established that the structure of perovskites ABO_3 is determined by the tolerance factor t . The evaluation of t for the $\text{Nd}_x\text{Ca}_{2-x}\text{FeMoO}_6$ ($x=0$ to $x=0.8$) series shows that it does not vary appreciably (from 0.869 to 0.871). Therefore, the observed conservation of crystalline symmetry outcomes as a natural result when considering the similar ionic radii between Nd^{3+} and Ca^{2+} , which leads to a nearly invariant tolerance factor in the studied doping range.

Structural details obtained from the joint Rietveld refinement of XRPD and NPD data are listed in Table I. Figure 1 displays lattice parameters and cell volume (normalized to that of $x=0$) obtained as a function of x . A monotonic expansion of both the cell parameters and cell volume is observed upon increasing the Nd-substitution. As this expansion cannot be attributed to steric effects, it has to be interpreted as a genuine signature of the effective doping of antibonding states on the Fe-Mo sublattice, which produces an enlargement in (Fe, Mo)-O bond distances.¹² It is very instructive to compare the cell expansion observed in the NCFMO case

TABLE I. Structural parameters and reliability factors obtained from the joint refinement of XRPD and NPD data at room temperature.

Sample	$x=0$	$x=0.2$	$x=0.4$	$x=0.6$	$x=0.8$
Space Group	$P 2_1/n$	$P 2_1/n$	$P 2_1/n$	$P 2_1/n$	$P 2_1/n$
$a(\text{\AA})$	5.4124(5)	5.4293(6)	5.4334(4)	5.4447(4)	5.4545(4)
$b(\text{\AA})$	5.5226(5)	5.5434(6)	5.5511(4)	5.5645(4)	5.5779(4)
$c(\text{\AA})$	7.7045(8)	7.7296(8)	7.7370(8)	7.7543(8)	7.7694(8)
$V(\text{\AA}^3)$	230.3(1)	232.7(1)	233.4(1)	235.0(1)	236.4(1)
AS(%)	6(2)	12(3)	14(3)	26(5)	32(6)
$\langle d_{(\text{Fe,Mo})-\text{O}}(\text{\AA}) \rangle$	1.99(2)	1.99(3)	1.99(3)	2.00(5)	2.01(6)
$\langle \theta_{\text{Fe,Mo-O}}(^{\circ}) \rangle$	153(1)	153(1)	153(1)	153(2)	152(2)
$R_B(\text{XRPD})$	3.7	8.9	4.3	4.8	4.2
$R_B(\text{NPD})$	3.2	3.1	3.1	3.7	4.6
χ^2	6.3	5.2	6.9	8.2	8.3

with the corresponding data [included in Fig. 1(b)] obtained for other electron doped DP's (LSFMO¹² and NSFMO¹¹): It can be appreciated that the expansion of unit cell volume is stronger in NCFMO than in LSFMO¹² and NSFMO.¹¹ This

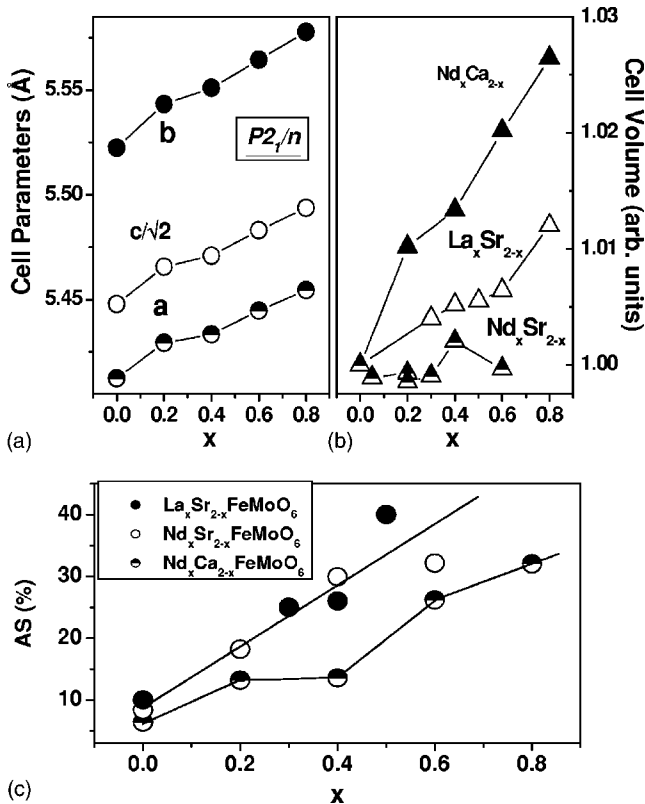


FIG. 1. (a) Evolution of the lattice parameters upon doping (x), for the $\text{Nd}_x\text{Ca}_{2-x}\text{FeMoO}_6$ series, as determined from XRPD. (b) Dependence of the cell volume with x , for the following series: $\text{Nd}_x\text{Ca}_{2-x}\text{FeMoO}_6$ (solid triangles), $\text{La}_x\text{Sr}_{2-x}\text{FeMoO}_6$ (open triangles) (Ref. 8) and $\text{Nd}_x\text{Sr}_{2-x}\text{FeMoO}_6$ (semi-open triangles) (Ref. 11). (c) Behavior of antisite concentration as a function of doping for $\text{Nd}_x\text{Ca}_{2-x}\text{FeMoO}_6$ (semi-open circles), $\text{La}_x\text{Sr}_{2-x}\text{FeMoO}_6$ (solid circles) (Ref. 8) and $\text{Nd}_x\text{Sr}_{2-x}\text{FeMoO}_6$ (open circles) (Ref. 11) series.

difference can be understood when taking into account the fact that $R_{\text{Ca}} \approx R_{\text{Nd}} < R_{\text{La}} < R_{\text{Sr}}$; it follows that the volume contraction upon La or Nd substitution in $\text{Sr}_{2-x}\text{A}_x\text{FeMoO}_6$ ($\text{A}=\text{La}, \text{Nd}$) competes with the cell expansion due to electron injection, thus reducing the rate at which the unit cell volume expands. Therefore, the NCFMO series presented in this paper permits to fully appreciate the structural effect (cell expansion) produced by band filling on Fe-Mo double perovskites, without the concomitant existence of structural distortions that may mask the influence of electron injection on the properties of the material. The volume expansion (about 2% for $x=0.6$) is close to what should be expected from the (Fe,Mo)-O bond expansion coefficient ($\Delta d/d \approx 0.5\%$ for $x=0.5$).¹² Notice that this variation ($\Delta d \approx 0.01 \text{ \AA}$) is smaller than the error bars in Table I.

Values printed in Table I show no appreciable variations of Fe-O-Mo bond angle upon doping. With this result we can assess that the change of this angle along the series, if any, is below the error bars (about 1°) and that it is much smaller than in other series (about 6° in $\text{La}_x\text{Sr}_{2-x}\text{FeMoO}_6$ between $x=0$ and $x=0.6$).¹² The electronic bandwidth (W) is given by $W \approx f(\theta)/d^{3.5}$ ²⁴ where $f(\theta)$ is some function of the bond angle and d its length. Therefore, being $f(\theta)$ constant, the bond expansion shall produce a relative change of W of only $\Delta W/W \approx 2\%$, thus justifying that our electronic system can be viewed as a rigid one.

In the ideal double perovskite, B/B' ions order in a rock-salt-like structure. However, it is usually found that Fe(Mo) ions get misplaced in Mo(Fe) sites. That is what is called an “antisite” (AS). In our convention, a perfectly ordered B/B' sublattice presents 0% of AS, while 50% of AS means a completely disordered one (that is, each B/B' position can be randomly occupied by an Fe or Mo ion). Figure 1(c) shows the concentration of antisites, as determined from XRPD Rietveld refinements, for the NCFMO series (semi-open circles). It is clear that AS increases with doping, as was also found for LSFMO¹² (solid circles) and NSFMO¹¹ (open circles) electron-doped samples. However, we shall point out that the antisites concentration all along the NCFMO series is systematically lower than that found in the case of LSFMO and NSFMO series, as can be seen in Fig. 1(c).

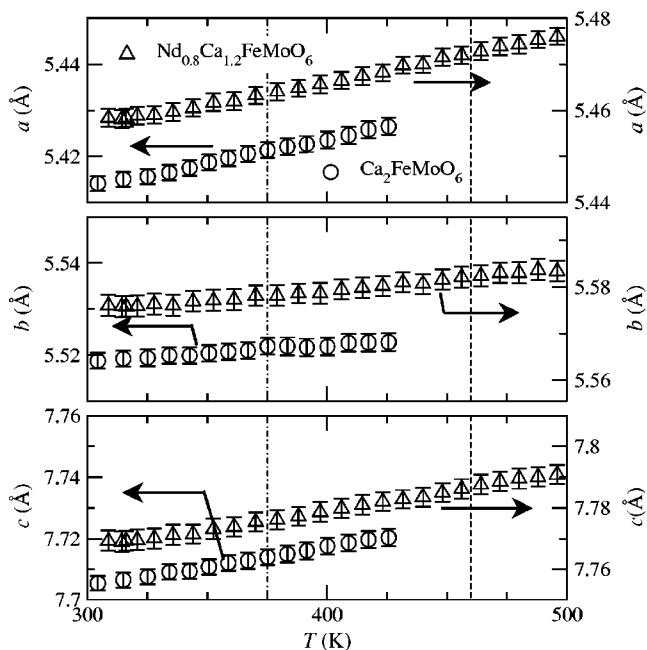


FIG. 2. Temperature evolution of lattice parameters of $x=0$ and $x=0.8$ compounds. Vertical lines are drawn at T_C (dashed line corresponds to $x=0.8$ and dot-dashed line to $x=0$).

From NPD data we have obtained the temperature evolution of cell parameters from RT to well above T_C . Figure 2 shows this evolution for $x=0$ and $x=0.8$ as case examples. Data have been successfully refined using $P2_{1/n}$ SG above and below T_C . It follows that in NCFMO there is not any structural transition associated to the onset of the ferromagnetic state. This observation is at difference with $\text{Sr}_2\text{FeMoO}_6$ compound, presenting a structural transition from cubic $Fm\bar{3}m$ to $I4/m$ at T_C .

B. NMR results

In a previous report on $^{95,97}\text{Mo}$ NMR investigations in $\text{Sr}_2\text{FeMoO}_6$ we have shown that Mo bears its own magnetic moment and that this moment is the only source of hyperfine field on Mo; due to the d character of the conduction band there is no transferred field mechanism and thus the magnetic moments of the neighbour atoms do not contribute to hyperfine field.¹⁷ Therefore, the NMR frequency is a direct measure of a magnetic moment on Mo, on grounds of the basic NMR relation:

$$\nu = \gamma H = \gamma A \mu,$$

where ν is the NMR frequency, γ is the nuclear gyromagnetic ratio of Mo, A is the hyperfine interaction constant, and μ is the magnetic moment of Mo ions. Consequently, Mo NMR frequency is a very sensitive probe of spin polarized charge around the Mo atom and can be used to monitor changes of spin and the related variation of the electric charge located in the $4d$ orbitals of Mo; even though the exact value of Mo magnetic moment μ cannot be extracted from these data due to the obscurity of the Mo hyperfine interaction constant A (see the discussion in Ref. 17).

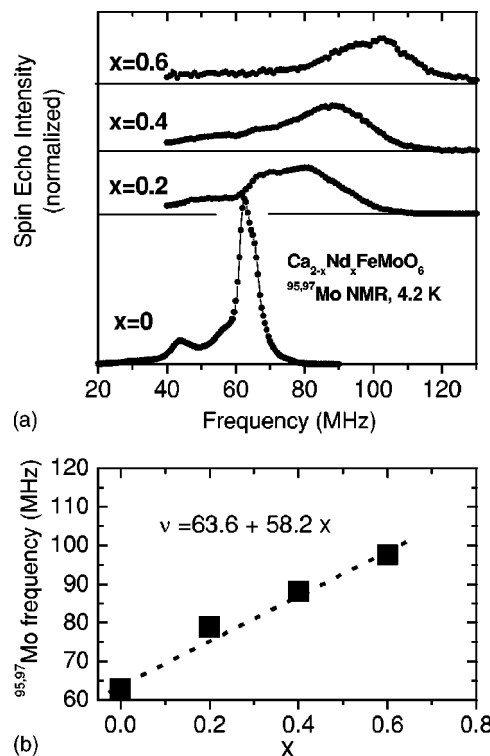


FIG. 3. (a) $^{95,97}\text{Mo}$ NMR spectra recorded at 4.2 K from $\text{Nd}_x\text{Ca}_{2-x}\text{FeMoO}_6$ ceramics, $0 \leq x \leq 0.6$. (b) $^{95,97}\text{Mo}$ NMR frequencies of the main line (ν) as a function of the Nd content (x) in $\text{Nd}_x\text{Ca}_{2-x}\text{FeMoO}_6$.

The $^{95,97}\text{Mo}$ NMR spectrum recorded at 4.2 K from pristine $\text{Ca}_2\text{FeMoO}_6$ (CFMO) [Fig. 3(a)—bottom panel] closely resembles that reported for the isoelectronic compound $\text{Sr}_2\text{FeMoO}_6$ (SFMO).¹⁷ The main NMR line at 63 MHz in case of CFMO corresponds to the Mo hyperfine field value of 22.5 T, which is about 6% less than the corresponding value in case of SFMO, indicating a proportionally smaller Mo magnetic moment and a smaller electric charge accumulated in the Mo orbitals. The low frequency structure in the Mo spectrum is similar to that observed in case of SFMO. A detailed NMR study carried out on a number of SFMO samples with a varying content of Fe-Mo antitesites (AS) has shown that this structure is totally insensitive to the amount of AS and thus it does not represent Mo atoms with the perturbed Fe-Mo environment,¹⁷ but it could be a signature of the charge instability proposed by Alonso and Sarma.^{20,21}

The effect of substitution of divalent Ca with trivalent Nd in $\text{Nd}_x\text{Ca}_{2-x}\text{FeMoO}_6$ on the NMR spectra is presented in Fig. 3(a) for $x=0.2, 0.4, 0.6$. While the principal spectrum characteristics, i.e., the main resonance line and the low frequency tail are preserved for all concentrations, two effects are clearly visible: The entire NMR spectrum is shifted towards higher frequencies and the lines become broader leading to a loss of resolution on the low frequency side. The position of the main NMR line, determined from a fit of a symmetric gaussian to the experimental intensity is plotted in Fig. 3(b). A linear increase of resonance frequency with increasing Nd concentration with a slope of 58.2 MHz per Nd atom is evident. That means that by replacing one Ca^{2+} with

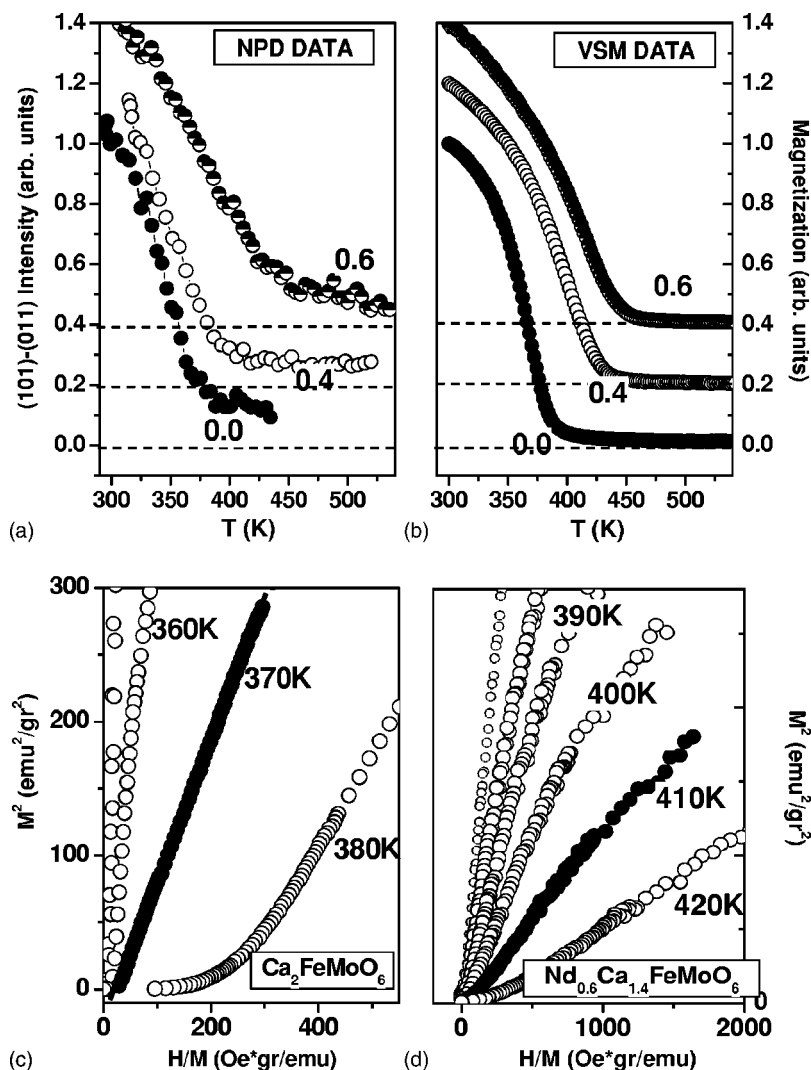


FIG. 4. (a) Evolution of the intensity of the (101)-(011) doublet with the temperature, as determined from NPD, for selected samples of the $\text{Nd}_x\text{Ca}_{2-x}\text{FeMoO}_6$ series. The zero is indicated by dashed lines, and has been shifted up when necessary, for sake of clarity. (b) Magnetization (1 kOe) as a function of the temperature for $\text{Nd}_x\text{Ca}_{2-x}\text{FeMoO}_6$ samples. (c) and (d) Isothermal field-dependent magnetization measurements (Arrot plots), for $\text{Ca}_2\text{FeMoO}_6$ and $\text{Nd}_{0.6}\text{Ca}_{1.4}\text{FeMoO}_6$, respectively. Curves showing the change of inflection (indicating thus the Curie temperature) are signaled in filled symbols.

Nd^{3+} ion, the hyperfine field on Mo is increased by about 92%. Since the magnetic moment of Mo is the only source of hyperfine field, this implies that the magnetic moment of Mo is almost doubled by replacing one Ca^{2+} with Nd^{3+} . In view of the invariance of the electronic structure resulting from the lack of steric effects, the observed increase of the magnetic moment has to be regarded as the filling of Mo-4d spin-down subband.

It is interesting to compare the observed effect of Nd^{3+} substitution in CFMO to a similar influence of La^{3+} doping in SFMO, which we have reported earlier.¹⁷ One can readily notice that the increase of NMR frequency (58.2 MHz/Nd) is slightly higher in case of Nd^{3+} substitution in CFMO compared to La^{3+} doping in SFMO (49.5 MHz/La). This may be related to the fact that in case of LSFMO system some steric effects cannot be excluded which would lead to a smaller effective field for the same concentration of the trivalent ion (La, Nd, respectively).

C. Magnetic properties

The determination of T_C is a key experimental issue, as noted in Ref. 18, and it was done by using different methods.

(i) From magnetization versus temperature $M(T)$ measurements (using a VSM apparatus, under a 1 kOe field) T_C was extracted from the extrapolation of the magnetization in the transition region to the region of zero magnetization [Fig. 4(b)]. (ii) Curie temperatures were also extracted from Arrot plots constructed from isothermal field-dependent magnetization measurements [data for some representative temperatures and samples are included in Figs. 4(c) and 4(d)]. (iii) Finally, Curie temperatures were also determined from neutron powder diffraction data, by following the evolution of the intensity of the (101)-(011) doublet [Fig. 4(a)], which is basically of magnetic origin. We shall stress that data in Figs. 4(a) and 4(b) clearly show that the onset of ferromagnetism of the NCFMO samples is shifted to higher temperatures as Nd concentration increases, irrespectively on the experimental tool used to determine it.

In Fig. 5 we collect the values of T_C extracted from data in Figs. 4(a)–4(d). Data in Fig. 5 indicate a robust rising of T_C upon doping, independently of the particular way it is obtained. Assuming a linear dependence of T_C on x we obtain dT_C/dx ratios of about 1.9 K/%Nd($M(T)$), 2.1 K/%Nd(NPD) and 1.6 K/%Nd (Arrot plots). Data in Fig. 4 also reveals that the magnetic transition broadens

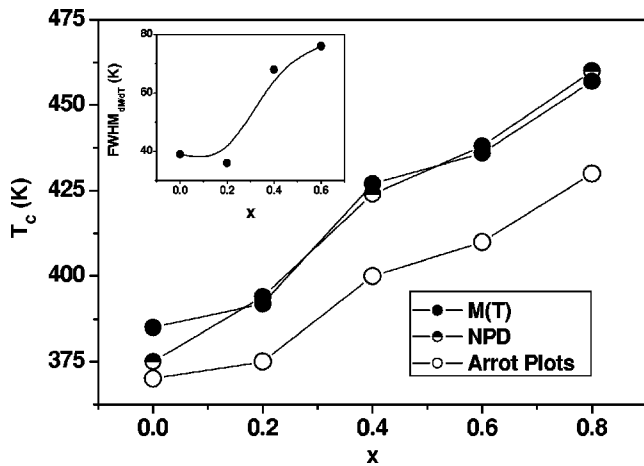


FIG. 5. (Main Panel) Curie temperatures as a function of doping (x), for the $Nd_xCa_{2-x}FeMoO_6$ series. (Inset) FWHM corresponding to the first derivative of $M(T)$ data, for the $Nd_xCa_{2-x}FeMoO_6$ series.

slightly when increasing the doping level; this observation can be better appreciated by determining the full width at half maximum (FWHM) of the first derivative of $M(T)$ data as shown Fig. 5 (inset). The broadening of the $M(T)$ transitions accounts for the observation of different dT_c/dx values when distinct techniques and criteria are used. Finally, we shall stress that the observed increase of the Curie temperature upon Nd-substitution can not be attributed to the progressive increase of AS upon doping, as it has been experimentally shown that the Curie temperature of Sr_2FeMoO_6 does not appreciably rise (or even lowers) when increasing the disorder up to 35% of AS.¹⁵

Figure 6(a) shows the magnetization versus field measurements (at 10 K) for NCFMO series (solid symbols). This figure clearly shows that, under doping, the magnetization of

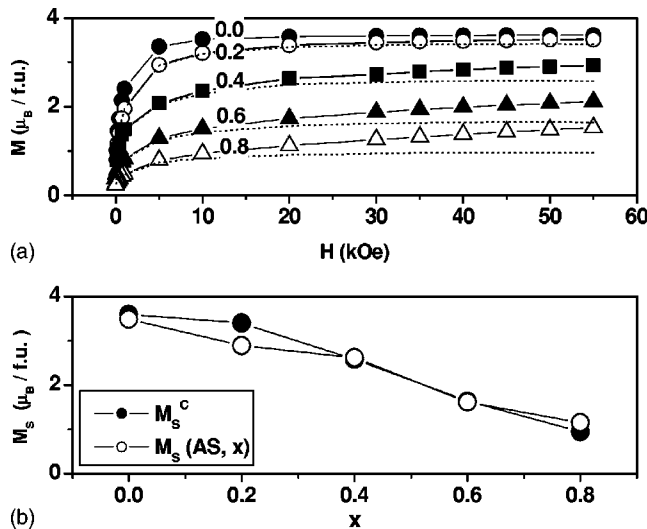


FIG. 6. (a) Magnetization as a function of field, for different $Nd_xCa_{2-x}FeMoO_6$ samples. Data was taken at 10 K. Dotted lines show the corrected magnetization after subtracting the contribution of paramagnetic Nd^{3+} ions. (b) Evolution of the corrected experimental saturation magnetization (M_s^c , solid circles), as well as the estimated value [$M_s(AS, x)$, as defined in the text] upon doping.

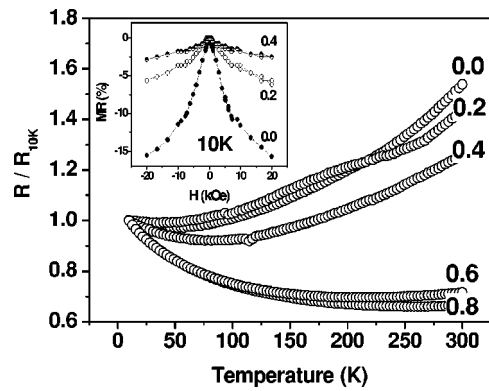


FIG. 7. (Main panel) Normalized resistivity as a function of temperature, for the $Nd_xCa_{2-x}FeMoO_6$ series. (Inset) Magnetoresistance as a function of the magnetic field for selected samples. Data were taken at 10 K.

the samples decreases. In addition, a differential susceptibility, manifested by the linear increase of magnetization with the magnetic field, progressively develops. As discussed in detail in Ref. 11, a similar behavior was observed in $Sr_{2-x}Nd_xFeMoO_6$ and it was argued that the high field susceptibility is dominated by the paramagnetic contribution of Nd^{3+} ions. The magnetization associated to the (FeMo) sublattice in NCFMO can be deduced after appropriate subtraction of the Nd-ions contribution as explained in Ref. 11. The corrected saturation magnetizations (M_s) obtained after discounting the paramagnetic Nd^{3+} contribution, are shown in Fig. 6(b) (solid symbols). The decrease of the saturation magnetization is well described by the simple model⁸ $M_s^c(AS, x) = 4(1-2AS)\mu_B - x(1-2AS)\mu_B$ where the first term accounts for the lowering of magnetic moment due to the existence of antisite disorder, and the second term corresponds to the reduction of magnetization due to the injection of electrons—by doping—on the “spin down” band. The calculated $M_s^c(AS, x)$ values are also shown in Fig. 4(b) (open symbols). The agreement between the experimental and the estimated saturation magnetizations is remarkably good. It is worth mentioning that the main contribution to the reduction of M_s^c comes from the presence of AS.

D. Transport properties

The evolution of resistivity with temperature of NCFMO samples is shown in Fig. 7 (main panel). A metallic-like behavior is observed for the pristine compound until about 50 K, where the temperature dependence flattens and an upturn is visible at lower temperatures. Data in Fig. 5 indicate that upon doping, the low-temperature insulating-like behavior becomes somewhat more important. It thus follows that Nd-doping induces a moderate detriment of metallicity of the samples. As investigated samples are ceramics the contribution of grain boundaries to the measured resistivity cannot be avoided; however, the monotonic dependence of the normalized resistivity on Nd contents (Fig. 7) suggests that it can be of intrinsic origin; it could be argued that the presence of Fe-Mo disorder (antisites) can be at the origin of the weakening of the metallic transport channel. As show in Fig. 7

(inset), the magnetoresistance (MR) (at 10 K) is gradually suppressed by the Nd doping.

A similar trend of resistivity and magnetoresistance upon La or Nd doping has been recently reported in LSFMO and NSFMO.^{8,11} Sarma *et al.*²⁵ have suggested that antisites in double perovskites may suppress the half-metallic character. Due to the fact that all electron-doped samples display a higher concentration of antisities, our results appear to be compatible with Sarma's suggestion.

IV. SUMMARY AND CONCLUSIONS

After presenting this overview of all results, we turn now back and focus our attention on the behavior of T_C of NCFMO series and its implications. We point out that we have observed a robust increase of T_C upon electronic doping and we have evidenced the carrier injection into Mo states by the increase of Mo hyperfine field. Moreover, the enhancement of T_C occurs in a system in which the electronic doping is achieved while steric effects are minimized, and the crystal symmetry is preserved upon atomic (Nd) substitution.

It is remarkable that the rate dT_C/dx we have determined for the Ca-substituted NCFMO [1.8(3)K/%Nd] is quite similar, although slightly larger, than those reported for Sr-substituted NSFMO series (1.6 K/%Nd)¹¹ or LSFMO series (1.3 K/%La).⁸ Moreover, the rate of Mo NMR frequency $d\nu/dx$ correlates with the above tendency (58.2 MHz/Nd in CFMO and 49.5 MHz/La in SFMO). This observation excludes that steric effects and the eventual change of symmetry (from $I4/m$ to $P2_{1/m}$) being relevant for the observed enhancement of T_C . We also note that the close similarity of dT_C/dx is at first sight, surprising and it could not have been anticipated on the basis of the model by Tovar *et al.*³ Indeed, it predicts that the strength of the ferromagnetic coupling is determined by the density of states ($D(E)$) at the Fermi edge.³ Therefore, unless the density of states close to the Fermi level or, more precisely, its variation upon band filling, are very similar in both $\text{Ca}_2\text{FeMoO}_6$ and $\text{Sr}_2\text{FeMoO}_6$ compounds, then substantially different values of dT_C/dx could be expected. The remarkable similarity of the experimental values of dT_C/dx thus indicates that differences in the density of states induced by the different alkalines (Sr, Ca) cannot be very significant. In agreement with this finding, Szotek *et al.*²⁶ have recently computed the electronic structure of ferromagnetic A_2FeMoO_6 and they have found that the density of states around the Fermi edge is very similar for both alkaline ions. Earlier calculations of the electronic band structure,²⁷ indicating critical differences between $D(E)$ of Sr and Ca DP's do not fit with the present results.

We thus conclude that our experimental data provide definitive evidence that the rise of T_C induced by trivalent ions substituting divalent ones, in double perovskites is essen-

tially a band filling effect and structural modifications, namely bond bending, have a minor role.

Finally, we would like to recall that, as mentioned in the introduction, attempts to predict theoretically a rise in T_C upon electron doping have failed.^{19,20} These models assume that doping occurs in a rigid-band system. As this requirement is almost perfectly fulfilled in the present $\text{Nd}_x\text{Ca}_{2-x}\text{FeMoO}_6$ series, the reason(s) for the dramatic discrepancy between theory and experiments shall be found elsewhere. J.L. Alonso *et al.*²⁰ argued that the microscopic reason for the predicted lowering of T_C is that in the models elaborated so far, the doping carriers occupy both (spin-up and spin-down) states. Therefore, one may speculate that suppression of electron filling of the wrong spin channel (spin-up) could be a way to circumvent the difficulty. A possible way to induce this effect could be the introduction of substantial electron correlations in the $4d(\text{Mo})$ states, pushing up the energy of the spin-up $4d(\text{Mo})$ states.²⁸

After submission of the manuscript we became aware that the oxides $\text{Ba}_{1+x}\text{Sr}_{1-3x}\text{La}_{2x}\text{FeMoO}_6$ has been recently prepared.²⁹ In this series the averaged ionic size of the species occupying the large cage of the perovskite unit, is kept constant and thus, to some extent, that series resembles the $\text{Ca}_{2-x}\text{Nd}_x\text{FeMoO}_6$ one reported here. We note, however, that due to the substantial differences in ionic radii of the Ba, Sr, and La ions, their ionic size variance is substantially larger and it changes along the series. From this point of view, the difference with our series is remarkable because in the $\text{Ca}_{2-x}\text{Nd}_x\text{FeMoO}_6$ case not only the ionic size of the lanthanide is constant but also its variance is kept constant and virtually zero. In spite of this, and in agreement with our results, the Curie temperature has been found to increase at rate of about ~ 1.32 K/La% with electron doping.

Summarizing, we have reported a detailed study of the structural, magnetic and transport properties of $\text{Nd}_x\text{Ca}_{2-x}\text{FeMoO}_6$. We have shown that although steric effects are absent and the symmetry of the structure is preserved upon Nd doping, the Curie temperature of these oxides rises at a rate of 1.8(3)K/%Nd. We have argued that this is a genuine band-filling effect that takes place in a rigid band system, and we have critically revised some assumptions in currently available models of ferromagnetic coupling in double perovskites.

ACKNOWLEDGMENTS

This work has been supported in part by F.P.-V of the E.C. under Contract No. G5RD-CT2000-00138 (AMORE) and by the MCyT (Spain) projects MAT2002-03431, MAT 2003-07483-C02-02 and FEDER. C. F. acknowledges financial support from MCyT and the Warsaw group acknowledges a grant from Ford Motor Company. Enlightening discussions with F. Guinea and L. Brey are very much appreciated.

- ¹K. I.-Kobayashi, T. Kimura, H. Sawada K. Terakura, and Y. Tokura, *Nature (London)* **395**, 677 (1998).
- ²B. Martinez, J. Navarro, Ll. Ballcells, and J. Fontcuberta, *J. Phys.: Condens. Matter* **12**, 10 515 (2000).
- ³M. Tovar, M. T. Causa, A. Butera, J. Navarro, B. Martinez, J. Fontcuberta, and M. C. G. Passeggi, *Phys. Rev. B* **66**, 024409 (2002).
- ⁴C. Ritter, M. R. Ibarra, L. Morellon, J. Blasco, J. García, and J. M. de Teresa, *J. Phys.: Condens. Matter* **12**, 8295 (2000).
- ⁵M. Besse, V. Cros, A. Barthélémy, H. Jaffrès, J. Vogel, F. Petroff, A. Mirone, A. Tagliaferri, P. Bencok, P. Decorse, P. Berthet, Z. Szotek, W. M. Temmerman, S. S. Dhesi, N. B. Brookes, A. Rogalev, and A. Fert, *Europhys. Lett.* **60**, 608 (2002).
- ⁶Y. Moritomo, Sh. Xu, A. Machida, T. Akimoto, E. Nishibori, M. Takata, and M. Sakata, *Phys. Rev. B* **61**, R7827 (2000).
- ⁷T. Dietl, *Semicond. Sci. Technol.* **17**, 377 (2002).
- ⁸J. Navarro, C. Frontera, Ll. Balcels, B. Martinez, and J. Fontcuberta, *Phys. Rev. B* **64**, 092411 (2001).
- ⁹D. Serrate, J. M. De Teresa, J. Blasco, M. R. Ibarra, and L. Morellón, *Appl. Phys. Lett.* **80**, 24 (2002).
- ¹⁰J. Lindén, T. Shimada, T. Motohashi, H. Yamauchi, and M. Karppinen, *Solid State Commun.* **129**, 129 (2004).
- ¹¹D. Rubi, C. Frontera, J. Nogués, and J. Fontcuberta, *J. Phys.: Condens. Matter* **16**, 3173 (2004).
- ¹²C. Frontera, D. Rubi, J. Navarro, J. L. García-Muñoz, J. Fontcuberta, and C. Ritter, *Phys. Rev. B* **68**, 012412 (2003).
- ¹³D. Sánchez, J. A. Alonso, M. García-Hernández, M. J. Martínez López, J. L. Martínez, and A. Møllergard, *Phys. Rev. B* **65**, 104426 (2002).
- ¹⁴H. M. Yang, W. YY. Lee, B. W. Lee, and C. S. Kim, *J. Appl. Phys.* **98**, 6987 (2003).
- ¹⁵J. Navarro, J. Nogués, J. S. Muñoz, and J. Fontcuberta, *Phys. Rev. B* **67**, 174416 (2003).
- ¹⁶J. Navarro, J. Fontcuberta, M. Izquierdo, J. Avila, and M. C. Asensio, *Phys. Rev. B* **69**, 115101 (2004).
- ¹⁷M. Wojcik, E. Jedryka, S. Nadolski, J. Navarro, D. Rubi, and J. Fontcuberta, *Phys. Rev. B* **69**, 100407 (2004).
- ¹⁸J. B. Philipp, P. Majewski, L. Alff, A. Erb, R. Gross, T. Graf, M. S. Brandt, J. Simon, T. Walthert, W. Mader, D. Topwal, and D. D. Sarma, *Phys. Rev. B* **68**, 144431 (2003).
- ¹⁹K. Phillips, A. Chattopadhyay, and A. J. Millis, *Phys. Rev. B* **67**, 125119 (2003).
- ²⁰J. L. Alonso, L. A. Fernández, F. Guinea, F. Lesmes, and V. Martín-Mayor, *Phys. Rev. B* **67**, 214423 (2003).
- ²¹D. D. Sarma, P. Mahadevan, T. Saha-Dasgupta, Sugata Ray, and A. Kumar, *Phys. Rev. Lett.* **85**, 2549 (2000).
- ²²J. Rodriguez Carvajal, *Physica B* **192**, 55 (1993).
- ²³J. A. Alonso, M. T. Casais, M. J. Martínez-Lopez, J. L. Martínez, P. Velasco, A. Muñoz, and M. T. Fernández-Díaz, *Chem. Mater.* **12**, 161 (2000).
- ²⁴W. A. Harrison, *Electronic Structure and Properties of Solids* (Freeman, San Francisco, 1980).
- ²⁵T. Saha-Dasgupta and D. D. Sarma, *Phys. Rev. B* **64**, 064408 (2001).
- ²⁶Z. Szotek, W. M. Temmerman, A. Svane, L. Petit, and H. Winter, *Phys. Rev. B* **68**, 104411 (2003).
- ²⁷T. S. Chan, R. S. Liu, G. Y. Guo, S. F. Hu, J. G. Lin, J. M. Chen, and J. P. Attfield, *Chem. Mater.* **15**, 425 (2003).
- ²⁸L. Brey (private communication).
- ²⁹D. Serrate, J. M. De Teresa, J. Blaco, L. Morellon, M. R. Ibarra, and C. Ritter, *Eur. Phys. J. B* **39**, 35 (2004).